THE RIGAKU JOURNAL
VOL. 19 / NO. 2 & VOL. 20 / NO. 1 / 2003

POWDER DIFFRACTION OF MODULATED AND COMPOSITE STRUCTURES

A. V. MIRONOV, A. M. ABAKUMOV AND E. V. ANTIPOV

Department of Chemistry, Moscow State University, Moscow 119899, Russia.
e-mail: mironov@icr.chem.msu.ru, abakumov@icr.chem.msu.ru, antipov@icr.chem.msu.ru

In the past two decades intensive development of the theory of $3+d$ dimensional crystallography, experimental techniques and corresponding software makes it possible to perform phase analysis and even structure refinement from powder diffraction data for modulated and composite structures. In the present paper the X-ray powder diffraction from such structures is considered. Two examples of multispace structure refinement of the modulated ($Bi_{2.3}Sr_{1.7}CuO_{6.23}$) and composite ($Sr_{1.32}Mn_{0.83}Cu_{0.17}O_3$) structures from conventional X-ray source data are presented.

1. Introduction

Numerous compounds are known, whose diffraction patterns require four (or more) integer Miller indexes to be indexed completely. Such compounds are said to have modulated structures, which can be interpreted as perturbations with respect to an average conventional structure. Reflections, which cannot be indexed with the usual three-dimensional unit cell, are called satellites. Fourth vector, namely the modulation vector, is introduced as a combination of reciprocal vectors (see Formalism, Eq. (1)), thus creating special cell set of four vectors, called vector modulo of order 4 in three dimensional space. The first indications that crystal structures may not exhibit normal lattice periodicity were found late in 19th century. Physically it means, that neighboring unit cells are not alike, but the deviation of each unit cell from an average structure can be described by a periodic function with its own period. The presence of such periodicity is proved by the existence of a diffraction pattern itself. The formalism of the description was suggested by P. M. de Wolff in 1974 [1]. Reflections that are predominantly strong are consistent with a regular 3-dimensional reciprocal lattice and are called main reflections, but others, called satellites do not fit the same lattice. On the other hand, while the satellites do not fully match the main lattice, the whole pattern can be described by vector modulo of order 4 in three dimensional space. Hence, it can be imagined that the 3-dimensional diffraction pattern is a projection of a $3+d$-dimensional reciprocal lattice, in which the main (R) and the satellite (S) reflections are all regularly situated at the lattice nodes (Fig. 1a). From the properties of the Fourier transform the incommensurate modulated structures are treated as $3+d$ dimensional and real structures can be depicted as three-dimensional sections R_3 of a multispace (Fig. 1b, c). Such $3+d$ unit cells retain the atomic periodicity with atoms represented as strings, while the three-dimensional structure is not periodic. On the other hand, diffraction methods reflect the average atomic distribution over a structure. Thus, the average three-dimensional structure can be treated as the summation of an electron density over additional dimensions (x_4 in the case of $3+1$ dimensional structure) and its projection on R_3. Obviously, the refinement of this type of structure will result in unreal atomic and/or structural parameters, like atomic displacement parameter(s) (ADP), interatomic distances or coordination polyhedra. If the behaviour of atoms along additional dimensions is described by a periodic function, it means, that exact atomic parameters for each unit cell can be calculated. If the ratio between the components of the modulation vector and cell parameter(s) is rational, a structure is called commensurate and can be described in terms of a superstructure, otherwise—this structure is referred to as incommensurate.

It should be stressed, that a structure remains three-dimensional and additional dimensions reflect any structural peculiarity, which the radiation source used is sensitive to. For neutrons it can be orientation of magnetic moments. For X-

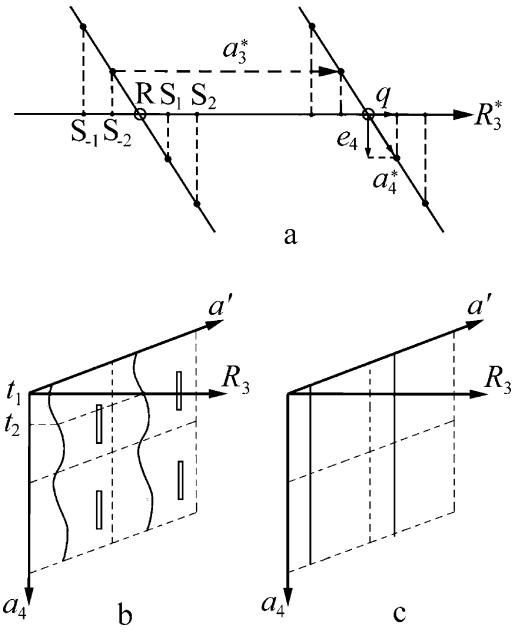

Fig. 1. Multispace presentation by P. M. de Wolff [1]: (a) Diffraction pattern, reciprocal space R_3^* – three-dimensional section of 3+1 reciprocal space, a_3^* and a_4^* – reciprocal cell vectors, R and S – main and satellite reflections respectively; (b) A structure with displacive and occupational modulations; (c) A structure with no modulations.

rays only positional, occupancy and ADP modulation of atoms are relevant.

Over the next years after P. M. de Wolff publication more stones were put in the foundation of multidimensional crystallography. Practical application of this method came to life. Two programs most commonly used for this purpose were developed: JANA* by V. Petriček and P. Coppens and REMOS† by A.Yamamoto, followed by other software‡. Late in 1980 s, first structures were refined from single crystal data with modulation parameters for heavy atoms only. Later light elements were included in this list. Nevertheless, many compounds are not easily grown as single crystals or the interesting phases present complex polydomain structures. Therefore, the study of a structure by single crystal techniques becomes very complicated, if possible. Rietveld refinement from neutron and/or X-ray data is the important step in the development of the multidimensional approach. X-ray powder diffraction from conventional sources is widely used in scientific studies. The correct interpretation of diffraction patterns is important for phase analysis and successive structure refinement. If unindexed peaks remain on a powder XRD pattern of a newly prepared compound, and other preparation routes produce materials having these peaks with similar relative intensities, the following problem should be considered: do extra lines correspond to an admixture, either the superstructure was not correctly taken into account or could they reflect the modulated or composite structure of a pure phase? If these extra lines correspond to satellite reflections of a modulated structure, then their intensities are relatively low. This is not the case for composite structures. Their diffraction patterns include at least two subsets of main reflections with intensities of one order of magnitude and thus, two sets of cell parameters can be refined. Does such a pattern belong to a two phase sample or the sample contains a single phase with the composite structure? In this review we would like to focus on such problems, using our own experience.

2. Short Notes on Formalism

The overwhelming majority of refined structures are described in four-dimensional space, so we will take it as an example. The theory of 3+d dimensional crystallography is described in details so far in many papers including the latest edition of *International Tables for Crystallography* [2]. We present here a brief description of the four-dimensional case.

The fourth basic vector $\boldsymbol{a}_4$, which is perpendicular to the $\boldsymbol{a}_1$, $\boldsymbol{a}_2$, $\boldsymbol{a}_3$ basic vectors of the R_3 direct space, is defined through a projection of corresponding reciprocal vector $\boldsymbol{a}_4^*$ (called modulation vector $\boldsymbol{q}$) in R_3^* reciprocal space (Fig. 1a):

$$\boldsymbol{q}=\sum_{i=1}^{3} k_i \boldsymbol{a}_i^* = \alpha \boldsymbol{a}^* + \beta \boldsymbol{b}^* + \gamma \boldsymbol{c}^* \qquad (1)$$

where at least one of the coefficients α, β and γ is irrational in general and possibly one or two are rational coefficients. Then, reciprocal cell vectors in R_4^* space are defined as: $\boldsymbol{a}_i'^* = \boldsymbol{a}_i^*$ for i=1–3 and $\boldsymbol{a}_4^* = \boldsymbol{q} + \boldsymbol{e}_4$, and from orthogonality condition:

$$\boldsymbol{a}_i' = \boldsymbol{a}_i - k_i \boldsymbol{e}_4, \quad k_i = \alpha, \beta, \text{ or } \gamma, \quad i=1\text{–}3 \quad \boldsymbol{a}_4 = \boldsymbol{e}_4 \qquad (2)$$

* The present development of the JANA2000 package is continued by V. Petriček and M. Dušek. Find the package at http://www-xray.fzu.cz/jana/jana.html

† Find the package at http://quasi.nims.go.jp/yamamoto/index.html

‡ For more information on the software go to http://www-xray.fzu.cz/sgip/aphome.html or http://www.ccp14.ac.uk/solution/incomm.htm

The modulation vector is presented by $\boldsymbol{q}=\boldsymbol{q}_i+\boldsymbol{q}_r$, where $\boldsymbol{q}_i$ and $\boldsymbol{q}_r$ are irrational and rational parts of a modulation vector. The positions of reflections are given by a diffraction vector:

$$\boldsymbol{H}=h\boldsymbol{a}^*+k\boldsymbol{b}^*+l\boldsymbol{b}^*+m\boldsymbol{q} \tag{3}$$

where *hklm* are four Miller indices of a reflection. Main reflections (R) correspond to m=0, satellite (S) are others (Fig. 1a).

Functions that describe modulation waves are usually expanded in Fourier series:

$$f^v=\mathrm{A}_0^v+\sum_{n=1}^{m}\mathrm{A}_{s,n}^v\sin(2\pi n x_4)+\sum_{n=1}^{m}\mathrm{A}_{c,n}^v\cos(2\pi n x_4) \tag{4}$$

where f^v is the actual x, y or z coordinate, occupancy or corresponding ADP, A_0^v – corresponding parameter of the average structure, $A_{s,n}^v$ and $A_{c,n}^v$ – modulation parameters. For some special cases the other functions were used, namely linear or saw-tooth function for displacive modulation [3]:

$$x=x_0+2*\boldsymbol{U}_x*\frac{(x_4-x_4^0)}{\Delta} \tag{5}$$

and the step function for occupancy modulation [4]:

$$p(x_4)=1 \qquad x_4\in\left\langle x_4^0-\frac{\Delta}{2},x_4^0+\frac{\Delta}{2}\right\rangle$$

$$p(x_4)=0 \qquad x_4\notin\left\langle x_4^0-\frac{\Delta}{2},x_4^0+\frac{\Delta}{2}\right\rangle \tag{6}$$

where $\boldsymbol{U}_x$ is the amplitude of modulation, Δ is the length of the interval, where the function is defined, and x_4^0 is the parameter of the function representing the center of the step.

Interatomic distances and coordination polyhedra are the most important information for chemists. Two aspects should be taken into account. First, neighboring atoms in the average structure may have different x_4 coordinates. Thus, the comparison of any atoms including interatomic distance calculation should be performed for the same R_3 section defined by the phase shift parameter t:

$$t=x_4-(\boldsymbol{q}\cdot\boldsymbol{r}) \tag{7}$$

where $\boldsymbol{q}$ is a modulation vector and $\boldsymbol{r}$ is a vector defining the position of an atom in the average structure. The modulated structure itself should be considered as a function of any structural parameter (positions, ADPs, distances) vs. t. Second, two neighbouring unit cells on the modulation curves do not correspond to nearest points but differ by some value $\Delta t=t_2-t_1$ (t_1 and t_2 at Fig. 1b). If we shift the structure along any cell vector by its length, Δt becomes equal to an appropriate component of the modulation vector.

In the case of a composite structure two or more subsystems can be identified, each having its own set of cell parameters and space group symmetry. Let us consider the case with two subsystems, when both of them have common a and b parameters and different c_1 and c_2. Each subsystem can be defined from common lattice vectors and modulation vector by interlattice matrices:

$$\begin{pmatrix}\boldsymbol{a}_v^*\\ \boldsymbol{b}_v^*\\ \boldsymbol{c}_v^*\\ \boldsymbol{q}_v\end{pmatrix}=W^v\cdot\begin{pmatrix}\boldsymbol{a}^*\\ \boldsymbol{b}^*\\ \boldsymbol{c}^*\\ \boldsymbol{q}\end{pmatrix} \tag{8}$$

where $\boldsymbol{a}^*, \boldsymbol{b}^*, \boldsymbol{c}^*, \boldsymbol{q}$ – are reciprocal cell vectors and modulation vector of the composite structure, W^v and $\boldsymbol{a}_v^*, \boldsymbol{b}_v^*, \boldsymbol{c}_v^*, \boldsymbol{q}_v$ – interlattice matrix (W^1 is usually unit and $\boldsymbol{a}^*, \boldsymbol{b}^*, \boldsymbol{c}^*, \boldsymbol{q}$ are reciprocal vectors of the first subcell), reciprocal cell vectors and modulation vector of the v subsystem. If W^2 is equal

$$W^2=\begin{pmatrix}1&0&0&0\\0&1&0&0\\0&0&0&1\\0&0&1&0\end{pmatrix} \tag{9}$$

then $c_2^*=\boldsymbol{q}_1$. Indices of a reflection in respect to a certain subsystem are defined by:

$$\begin{pmatrix}h_v\\ k_v\\ l_v\\ m_v\end{pmatrix}=[(W^v)^{-1}]^{\mathrm{T}}\cdot\begin{pmatrix}h\\ k\\ l\\ m\end{pmatrix} \tag{10}$$

For the example given above the main reflections of the first subsystem have *hkl*0 indices, while *hk*0*m* reflections are the main reflections for the second one. Reflections with *hklm* indices are satellites for both subsystems. Thus, cell parameters of each subsystem can be refined using conventional approach, if necessary, but satellite reflections still can not be indexed in any subsystem using three-dimensional approach.

Symmetry of the 3+1 dimensional modulated

structures is described by four-dimensional space group [2, 5]. In general, each symmetry operation $(R, \varepsilon | \boldsymbol{t}, \tau)$ in the superspace implies ($R-3\times 3$ rotational matrix, $\boldsymbol{t}$ – translational vector of a symmetry operation, ε and τ refer to the additional dimension):

(1) Rotational and translational parts $(R|\boldsymbol{t})$ of the symmetry operation belong to the three-dimensional space group of the average structure;

(2) Point group operation R must keep the orientation of the modulation vector invariant. Thus, the value of ε is defined by the equation, often called de Wolff equation: $R\boldsymbol{q}_i - \varepsilon\boldsymbol{q}_i = 0$, or $\varepsilon\boldsymbol{q}_i = R\boldsymbol{q}_i$ (index i means irrational part of the modulation vector);

(3) If two atoms ν, η are related by a symmetry operation $(R|\boldsymbol{t})$ in the average structure, their modulation parameters are related as follows:

$$u^{\eta}(x_4) = Ru^{\nu}[\varepsilon(x_4 - \tau)] \tag{11}$$

$$p^{\eta}(x_4) = p^{\nu}[\varepsilon(x_4 - \tau)] \tag{12}$$

where $u(x_4)$ is the modulation function of coordinates, $p(x_4)$ is the occupancy modulation function. Non-zero translational part τ is associated with $\varepsilon = 1$.

Equations (11) and (12) should be satisfied if atoms ν and η coincide, that is for atoms in special positions, thus putting restrictions on the form of a modulation function. For example, in the case of one harmonic function either *sin* or *cos* waves (if any) should be used, depending on ε.

For composite structures the symmetries of both subsystems are defined by:

$$R_i^{\nu} = W^{\nu} R_i (W^{\nu})^{-1} \tag{13}$$

$$\boldsymbol{t}_i^{\nu} = W^{\nu} \boldsymbol{t}_i \tag{14}$$

where R_i^{ν} is the 4×4 rotational matrix of a symmetry operation and $\boldsymbol{t}_i^{\nu}$ is the translational part. The subsystems interact, giving rise to modulations of atoms, which are described in respect to their own bases. In addition to main reflections of undistorted subsystems, then satellite reflections occur. In general, such a structure can be described in one subsystem like a modulated structure, but in this case modulations of atoms from the second subsystem will be too large and nonharmonic. A detailed description of a composite structure approach is given in reviews (e.g. S. van Smaalen [6]).

3. Powder X-ray Diffraction Patterns

Powder XRD patterns of incommensurate modulated phases have several specific features, which have to be taken into account for successful extraction of information on the unit cell of the average structure and components of modulation vector. The *hklm* reflections on powder XRD patterns of incommensurate modulated phase form a dense set being projected on the 2θ axis, whereas for non-modulated or commensurate crystals this set becomes discrete. A profile decomposition and Rietveld refinement in the incommensurate case become possible because in most cases the intensities of satellite reflections quickly vanish with increasing order (i.e. with increasing $|m|$) that allows to consider the set of reflections as finite. In the majority of cases only first order satellites are visible on conventional powder XRD patterns. The restriction of maximal value of $|m|$ allows to assign indexes for satellite reflections. On the other hand, frequent overlapping of weak satellites with intense main reflections and generally low peak to background noise ratio for satellite reflections strongly restrict the accuracy in the positions of the satellites that can be determined from the experimental profile. Unfortunately poor quality data are usually available from conventional powder XRD pattern for determination and subsequent refinement of the components of the modulation vector. Up to now there is no reliable method, which can help to distinguish a modulated structure and determine a modulation vector from powder data. "...Powder indexing works beautifully on good data, but with poor data it will usually not work at all..." ("Data accuracy for powder indexing" – R. Shirley – NBS Spec. Publ. 567 (1980)), and, in agreement with this statement, a knowledge on three-dimensional reciprocal lattice is still needed for unambiguous determination of length and orientation of the modulation vector in reciprocal space. Selected area electron diffraction in a transmission electron microscope appears to be particularly useful for this purpose since it allows one to observe reciprocal space sections produced by diffraction from small areas of tens nanometers, i.e. from single crystallites from which the powder sample is formed. From the set of such electron diffraction patterns with known mutual orientations a full reconstruction of the three-dimensional reciprocal lattice can be performed. Let us consider several examples of indexing of such patterns. In Fig. 2 the [010] electron diffraction pattern of $Bi_{2.3}Sr_{1.7}CuO_{6.23}$ is shown. The rectangle marks the reciprocal unit cell corresponding to the average structure with the

monoclinic $A2/a$ space symmetry. The satellite reflections form rows assigned to each basic spot; the satellites can be indexed with the modulation vector $\boldsymbol{q}=0.22\boldsymbol{a}^*+0.61\boldsymbol{c}^*$. The α and γ components of the modulation vector were used then for indexing of powder XRD pattern based on peak positions calculated according to the formula (the monoclinic angle β is equal to 90°):

$$1/d^2_{hklm}=(h+m\alpha)^2/a^2+k^2/b^2+(l+m\gamma)^2/c^2$$

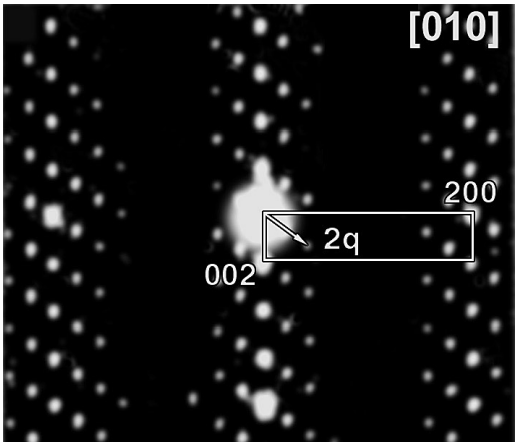

Fig. 2. [010] electron diffraction pattern of $Bi_{2.3}Sr_{1.7}CuO_{6.23}$.

Cell parameters and components of the modulation vector could be refined with standard least-squares procedure, as it is done, for example, in the CSD package [7]. For the $Bi_{2.3}Sr_{1.7}CuO_{6.23}$ phase it gives $\boldsymbol{q}=0.217(1)\boldsymbol{a}^*+0.608(1)\boldsymbol{c}^*$, in a good agreement with the electron diffraction data. The indexation of the XRD pattern for $Bi_{2.3}Sr_{1.7}CuO_{6.23}$ (PDF 45-0315) with four *hklm* indexes is present in Table 1.

For composite structures two sets of cell parameters should be determined, each belongs to its own subsystem. A separation of reflections belonging to the two main sets becomes easier if the XRD or electron diffraction patterns of both incommensurate and commensurate composite structures are available. A comparison of electron diffraction patterns of $Sr_{4/3}Mn_{2/3}Cu_{1/3}O_3$ and $Sr_{1.32}Mn_{0.83}Cu_{0.17}O_3$ compounds is shown in Fig. 3. This structures consist of two modulated subsystems, namely $[(Mn,Cu)O_3]_\infty$ and $[Sr]_\infty$, which have trigonal lattices with common parameter $a\approx9.6$ Å and different parameters $c_1\approx2.6$ Å and $c_2\approx3.9$ Å. The modulation vector can be chosen as $\boldsymbol{q}=c_1/c_2\boldsymbol{c}_1^*$. The structure of $Sr_{4/3}Mn_{2/3}Cu_{1/3}O_3$ is commensurate (that is $\boldsymbol{q}=2/3\boldsymbol{c}^*$), then it can be considered as a superstructure with $c\sim3\times2.60$ Å$=2\times3.90$ Å$=7.80$ Å. For the $Sr_{1.32}Mn_{0.83}Cu_{0.17}O_3$ the $c_1/c_2=0.662$ value requires a large denominator to be approximated by a rational number, and the structure is con-

Table 1. X-ray powder diffraction pattern of $Bi_{2.3}Sr_{1.7}CuO_{6.23}$ (PDF 45-0315). The deviations $\Delta\theta=\theta_{exp}-\theta_{calc}$ do not exceed 0.05°.

d	I/I_{100}	*hklm*	*d*	I/I_{100}	*hklm*
12.279	6	0 0 2 0	2.4092	7	$\bar{2}$ 0 2 $\bar{1}$, 1 2 0 0
5.262	7	0 1 1 0	2.3947	1	0 2 4 1
4.4773	1	0 0 6 $\bar{1}$	2.3654	1	1 2 2 0
4.0911	13	0 0 6 0	2.3532	<1	1 1 7 1
3.7678	3	1 1 1 0	2.3118	<1	2 1 3 0
3.6271	<1	0 1 5 0	2.3017	<1	0 1 9 1
3.6021	2	$\bar{1}$ 1 3 1	2.2512	1	2 0 6 0
3.4546	90	1 1 3 0	2.2447	1	1 2 4 0
3.3387	2	1 1 1 1	2.0773	2	1 2 6 0, $\bar{2}$ 0 8 1
3.2444	2	$\bar{1}$ 1 3 $\bar{1}$	2.0459	3	0 0 12 0
3.0669	22	0 0 8 0	2.0244	18	2 0 8 0
3.0098	94	1 1 5 0	2.0086	2	2 2 0 $\bar{1}$
2.9780	5	2 0 2 $\bar{1}$	1.9982	2	2 2 2 $\bar{1}$
2.9175	4	$\bar{1}$ 1 5 $\bar{1}$	1.9617	1	$\bar{2}$ 0 8 $\bar{1}$
2.8440	1	1 1 7 $\bar{1}$	1.9252	7	1 1 11 0
2.6947	100	2 0 0 0	1.9058	26	2 2 0 0
2.6312	2	2 0 2 0	1.8136	1	2 0 10 0
2.5808	5	1 1 7 0	1.8037	2	2 2 0 1
2.4675	1	2 0 4 0	1.7957	3	$\bar{2}$ 2 2 $\bar{1}$
2.4547	3	0 0 10 0	1.7611	1	$\bar{3}$ 1 3 1
2.4270	6	2 0 0 1			

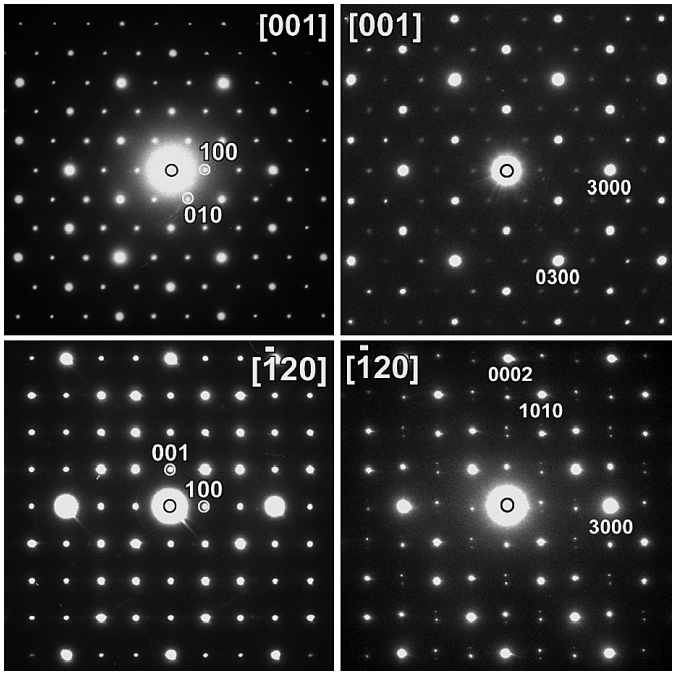

Fig. 3. Electron diffraction patterns of $Sr_{4/3}Mn_{2/3}Cu_{1/3}O_3$ (left column) and $Sr_{1.32}Mn_{0.83}Cu_{0.17}O_3$ (right column).

sidered as incommensurate. Deviation from being commensurate causes clear splitting of the satellite *hklm* reflections on the [$\bar{1}$20] electron diffraction pattern of $Sr_{1.32}Mn_{0.83}Cu_{0.17}O_3$ phase, while the *hkl*0 (from the $[(Mn, Cu)O_3]_\infty$) and *hk*0*m* reflections (from the $[Sr]_\infty$) remain unsplit on the [$\bar{1}$20] patterns of both $Sr_{4/3}Mn_{2/3}Cu_{1/3}O_3$ and $Sr_{1.32}Mn_{0.83}Cu_{0.17}O_3$ phases. The indexation scheme of the electron diffraction pattern of $Sr_{1.32}Mn_{0.83}Cu_{0.17}O_3$ phase is shown in Fig. 4, the indexation of powder XRD patterns is given in Table 2. This indexation can be compared with that of the commensurate $Sr_{4/3}Mn_{2/3}Cu_{1/3}O_3$ phase (a=9.5928(8) Å, c=7.8167(6) Å, S.G. P321, Table 3). The details on the $Sr_{1.32}Mn_{0.83}Cu_{0.17}O_3$ structure are described below.

After indexation the set of *hklm* reflections can be analyzed for the presence of systematic extinctions, and a (3+1)*d* superspace symmetry group (or several possible symmetry groups) can be proposed based on results of this analysis. This step-by-step procedure in the (3+1)*d* case is given in of *International Tables for Crystallography* [2] together with a list of (3+1)*d* superspace symmetry groups.

The correctness of the unit cell, modulation vector and superspace symmetry can be verified by the structure refinement. As well as for

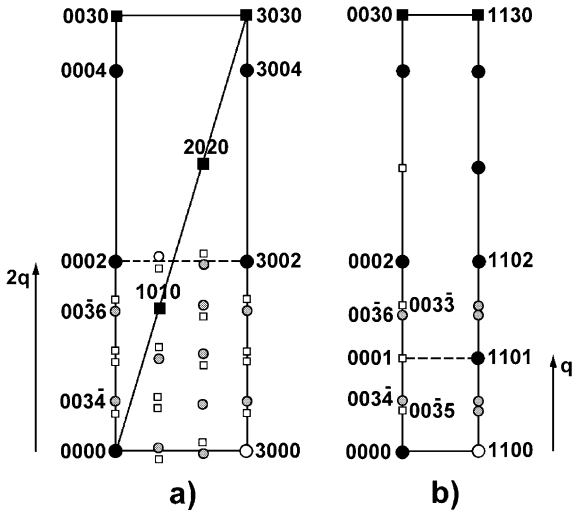

Fig. 4. Indexation of [$\bar{1}$20] (a) and [$\bar{1}$10] (b) ED patterns of the incommensurate $Sr_{1.32}Mn_{0.83}Cu_{0.17}O_3$ phase. Solid and dashed lines outline the unit cells of the $[(Mn, Cu)O_3]_\infty$ and $[Sr]_\infty$ subsystems, respectively. Black circles, black squares, open circles, gray circles and open squares mark the reflections of the $[Sr]_\infty$ subsystem, the $[(Mn, Cu)O_3]_\infty$ subsystem, common for both subsystems, satellites and reflections caused by double diffraction, respectively.

Table 2. X-ray powder diffraction pattern of $Sr_{1.32}Mn_{0.83}Cu_{0.17}O_3$. The deviations $\Delta\theta=\theta_{exp}-\theta_{calc}$ do not exceed 0.05°. Reflections with indices in two subsets are common for both subsystems. Only reflections with $I/I_{100}\geq 1\%$ are shown.

d	I/I_{100}	$[(Mn, Cu)O_3]_\infty$ subsystem	$[Sr]_\infty$ subsystem	Satellites
5.7762	3			1 0 1 $\bar{2}$
4.7961	3	2 $\bar{1}$ 0 0	2 $\bar{1}$ 0 0	
3.6904	1			0 2 1 $\bar{2}$
3.0397	84		1 1 0 1	
2.7696	100	3 0 0 0	3 0 0 0	
2.4811	1	1 0 1 0		
2.3986	2	4 $\bar{2}$ 0 0	4 $\bar{2}$ 0 0	
2.3041	2			1 3 $\bar{2}$ 3
2.2141	3			1 3 1 $\bar{2}$
2.2049	15	2 $\bar{2}$ 1 0		
2.0475	57		2 2 0 1	
2.0201	1			1 3 $\bar{1}$ 3
2.0105	1			4 0 1 $\bar{2}$
2.0026	14	3 $\bar{1}$ 1 0		
1.9643	11		0 0 0 2	
1.8553	1			2 3 $\bar{1}$ 2
1.8505	2			2 3 $\bar{1}$ 1
1.8181	6		1 1 0 2	
1.7246	4	4 $\bar{3}$ 1 0		
1.6466	18		1 4 0 1	
1.6033	10		3 0 0 2	
1.5996	18	6 $\bar{3}$ 0 0	6 $\bar{3}$ 0 0	

Table 3. X-ray powder diffraction pattern of $Sr_{4/3}Mn_{2/3}Cu_{1/3}O_3$. The deviations $\Delta\theta=\theta_{exp}-\theta_{calc}$ do not exceed 0.05°. Only reflections with $I/I_{100}\geq 1\%$ are shown.

d	I/I_{100}	*Hkl*
5.7008	5	1 0 1
4.7985	3	1 1 0
3.6692	2	2 0 1
3.5351	4	1 0 2
3.0305	100	1 1 2
2.7693	80	3 0 0
2.4846	2	1 0 3
2.3981	2	2 2 0
2.2926	1	3 1 0
2.2082	18	2 0 3
2.0442	50	2 2 2
2.0052	15	2 1 3
1.9847	1	3 1 2
1.9547	17	0 0 4
1.8970	5	3 0 3
1.8516	2	3 2 1
1.8099	14	1 1 4
1.7260	3	3 1 3
1.6447	15	4 1 2
1.6242	2	5 0 1, 4 0 3
1.5977	21	3 3 0

the Rietveld refinement of conventional structures, the initial model for modulated structure comprising atomic coordinates of the average structure and the starting parameters of modulation waves should be defined prior to the refinement. The initial model can be taken from a modulated structure of a similar compound, which was determined earlier from single crystal data, or derived from general structural and chemical considerations, which also can impose several sensible restrictions on the modulated functions thus decreasing a number of refineable parameters. Two such examples of Rietveld refinement of modulated structures are discussed below.

4. Incommensurate Modulated Superconducting Bismuth and Copper Mixed Oxides

Bismuth and copper mixed oxides were first synthesized by B. Raveau with co-workers [8]. Some of these substances were observed to exhibit superconducting properties, which resulted in extensive study of these compounds. The problem of the structure determination and refinement occurred at once due to significant modulations in their structures.

Bi-containing layered copper oxides $Bi_2Sr_2Ca_{n-1}Cu_nO_{2n+4+\delta}$ (n=1–3) have an intergrowth structure with perovskite and rock salt fragments alternating along the c axis (Fig. 5). They have an incommensurate modulated structure, and the appearance of modulation is associated with a mismatch between the BiO layer and perovskite-like fragment. This mismatch is reduced via strong shifts of atoms in all layers from ideal sites and insertion of additional oxygen atoms in the bismuth-containing layer. This model was suggested by H. Zandbergen *et al.* [9] and later proved by numerous studies.

An influence of modulations on a distribution of scattering density in Bi-2201 (n=1) phases is illustrated by a comparison of two high-resolution electron microscopy images. These

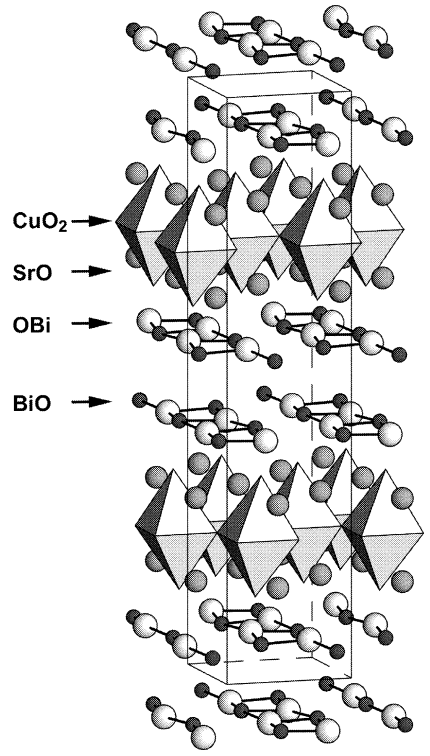

Fig. 5. Average structure of $Bi_{2.3}Sr_{1.7}CuO_{6.23}$ (2201 phase). Small dark-gray circles–Bi, large gray circles–Sr, large white circles–oxygen, extra oxygen atoms are not shown. Cu atoms are situated in the octahedra.

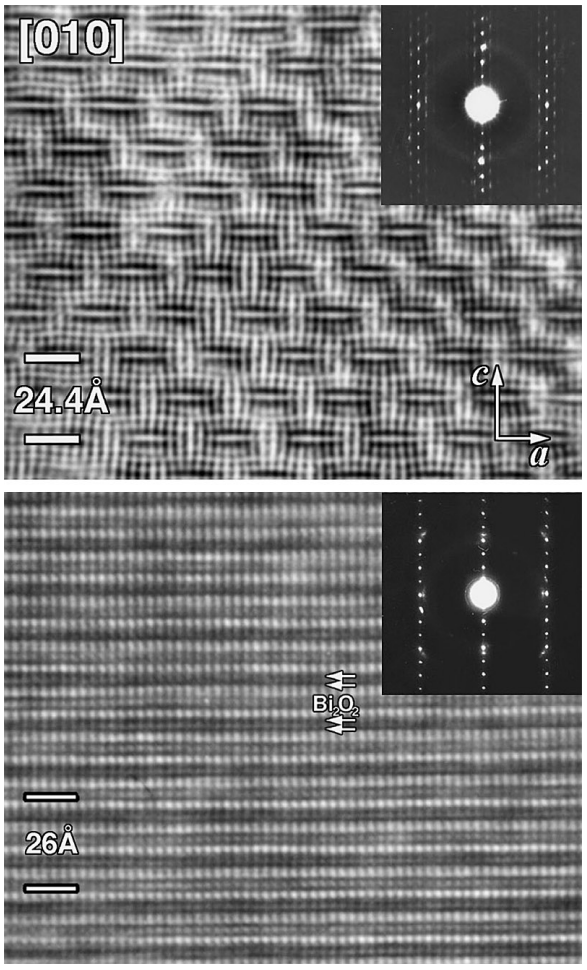

Fig. 6. HREM images of modulated $Bi_2Sr_{1.6}La_{0.4}CuO_{6.33}$ phase (top) and the same phase after fluorination (bottom). The corresponding electron diffraction patterns are shown as an inset. Note absence of satellite reflections on the electron diffraction pattern of the fluorinated phase.

images show the BiO layers in the modulated $Bi_2Sr_{1.6}La_{0.4}CuO_{6.33}$ phase (Fig. 6, top) and in the same phase after strong fluorination, where the modulations are suppressed by fluorine insertion into the BiO slabs (Fig. 6, bottom) [10]. Apparently, the structure refinement of Bi-2201 phase without modulations should result in a rough model with very large atomic displacement parameters especially for Bi atoms and unrealistic long Bi–O distances. The location of extra oxygen cannot be revealed within such model. The refinement of incommensurate modulated structures was successfully made from single crystal data [11–13]. However, it is very difficult to grow single crystals of Bi containing cuprates with desired composition. Several studies were performed using powerful sources such as neutron TOF or/and synchrotron radiation to obtain powder data and structures were refined [14, 15]. Although satellite reflections are much weaker than main reflections, their maximum intensities may be as high as 5–10% (relative scale). The significance is, that structure refinement from powder data without taking modulations into account can result in poor agreement factors. Now we consider the refinement of modulated bismuth cuprates from powder data and compare results with single crystal refinement. Sample preparations and data collections are described previously [16, 17]. The structures were refined using JANA2000 program package [18, 19].

A powder sample with the composition $Bi_{2.3}Sr_{1.7}CuO_{6.23}$ was used in this study. The 2201 phases crystallize in $A2/a(\alpha 0\gamma)$ monoclinic superspace group with pseudotetragonal cell parameters: $a \approx 5.4$ Å, $c \approx 24.5$ Å. First, the average structure was refined with the initial parameters taken from Leligny *et al.* [20]. Strontium site was supposed to be occupied by Sr and Bi with

a 0.85 : 0.15 ratio. The refinement converged only with a very low damping factor, fixed x coordinates for Bi and Sr atoms, and resulted to poor agreement with the experimental and calculated data (R_F=0.096, R_p=0.112). Such result was expected, because there are about 20–25 satellite reflections below 2θ=50° (for CuKα_1 radiation), which can be detected by profile decomposition of the pattern.

In incommensurate structure refinements several reliability factors are calculated according to the separation of the reflections into the group of main reflections and the groups of satellites of different order. R_F or R_I factors should be defined for each set of reflections. In general, satellite peaks are characterized by low peak to background ratios. This characterization leads to a significant effect on integral intensities of the satellites by the background noise and to larger reliability factors for these sets of reflections, even if the structure model is correct. Only first order satellites were used in the refinement of modulation parameters, higher order satellites have too low an intensity in the powder pattern and their intensities were not detected with profile analysis.

Displacive modulation parameters (one harmonic) for Bi atom were introduced in the refinement, resulting in a significant reduction of residuals: R_{F0}=0.072, R_{Fm}=0.052, R_{F1}=0.088, R_p=0.087 (here and further on index 0 stands for overall, m – for main reflections, 1 – for first order satellite reflections). Starting parameters for modulation were also taken from Leligny *et al.* [20]. Modulation parameters for other cations were then refined. Introduction of one harmonic for displacive modulation of all cations resulted in R_{F0}=0.049, R_{Fm}=0.036, R_{F1}=0.060, R_p=0.073. The refinement of the second harmonic revealed significance over 3σ only for Bi modulation parameters and along x_3 for Sr. At this stage R-factors were reduced to R_{F0}=0.039, R_{Fm}=0.027, R_{F1}=0.049, R_p=0.068. ADPs for all oxygen atoms were fixed to U_{iso}=0.025 and were not refined. For oxygen modulation refinement the model suggested in [21] was used. Modulations of oxygen atom in CuO_2 layer were refined with a harmonic function only. For other oxygen atoms (in the BiO and SrO layers) more complicated scheme was chosen. Modulations along x_1 were refined by a linear function with Δ=1 , while along x_2 and x_3 were left harmonic. Additional oxygen atom in BiO layer was not included into the refinement since its impact in powder XRD pattern is too small to be properly taken into account. The refinement converged only with low damping factor and reduced R-factors to R_{F0}=0.036, R_{Fm}=0.026, R_{F1}=0.045, R_p=0.065. Experimental, calculated and difference powder patterns are presented at Fig. 7.

The results of the refinement of the modulation functions for heavy scattering cations are very similar to those obtained from single crystal data for $Bi_{2.26}Sr_{1.74}CuO_{6.19}$ [21]. Amplitude of

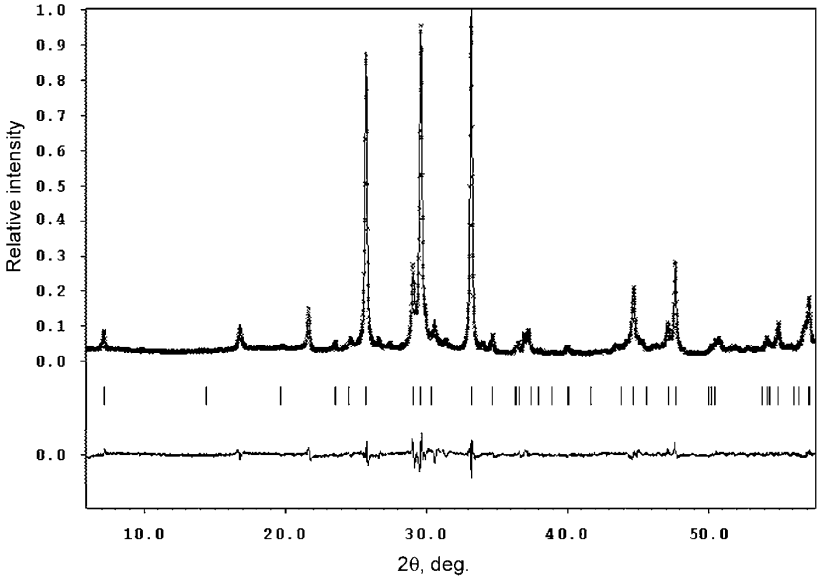

Fig. 7. Experimental, calculated and difference powder XRD patterns for $Bi_{2.3}Sr_{1.7}CuO_{6.23}$. Ticks mark the position of the main $hkl0$ reflections.

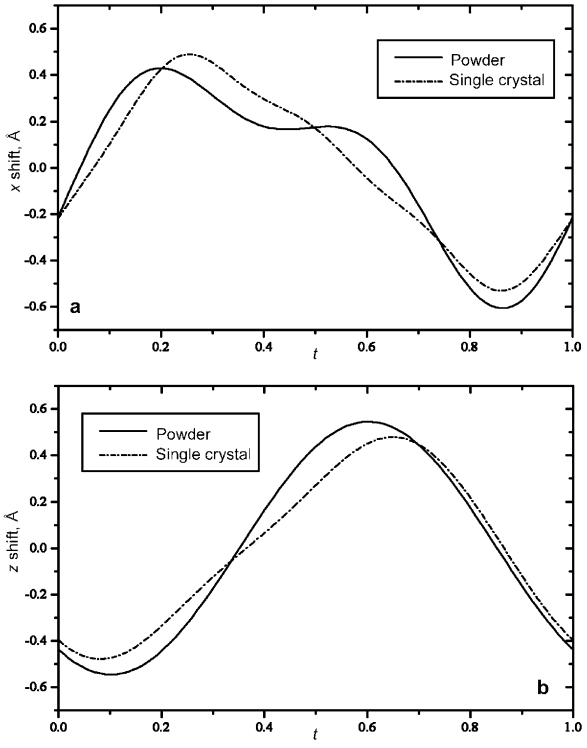

Fig. 8. Displacive modulation along *x* for Bi (a) and along *z* for Cu (*b*) in $Bi_{2.3}Sr_{1.7}CuO_{6.23}$.

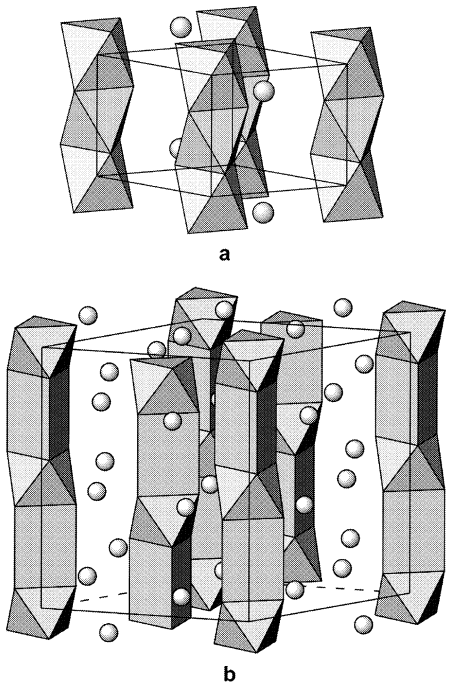

Fig. 9. Crystal structures of two $A_{3m+3n}A'_nB_{3m+n}O_{9m+6n}$ parent compounds: a) $m=1$, $n=0$; b) $m=0$, $n=1$.

modulations and *t* regions with maximal shift are essentially the same, some examples are presented at Fig. 8. As a result we may state, that the refinement of modulated structure from X-ray powder data produces a rough model of structural modulation. It reflects the general tendency and may be used for indexing of powder data, but exact atomic parameters and distances are the rough approximation of the real structure. The importance of such refinement is connected with full indexing of a diffraction pattern. The situation can be significantly improved if structural constrains are used in the refinement. In comparison with a single crystal X-ray diffraction experiment, X-ray powder patterns provide only information on a much smaller amount of structure amplitudes. Therefore, the number of refineable structure parameters should be restricted to those, which are very essential for the structure description. Now we will consider such approach for the composite $Sr_{1.32}Mn_{0.83}Cu_{0.17}O_3$ structure.

5. $Sr_{1+x}(Mn, Cu)O_3$ Hexagonal Perovskite Based Oxides with Chain Structures

$Sr_{1.32}Mn_{0.83}Cu_{0.17}O_3$ belongs to the family of hexagonal perovskite based oxides with the common formula $A_{3m+3n}A'_nB_{3m+n}O_{9m+6n}$. The structure of these oxides is generally considered as a derivative of the 2H hexagonal perovskite ABO_3 (Fig. 9a) that is based on the (*hh*) close packing of the (A_3O_9) layers. This structure consists of infinite chains of face-shared BO_6 octahedra with columns of A cations in between forming a hexagonal array in the $a=a_{per}\sqrt{2}$, $c=(2/\sqrt{3})a_{per}$ unit cell. One third of the oxygen atoms can be removed from the (A_3O_9) layers in an ordered manner, so that one trigonal prismatic cavity is created instead of two face sharing octahedral polyhedra (Fig. 9b). Additional A′ cations can be located inside these trigonal prisms resulting in a ($A_3A'O_6$) layer composition. The ordered alternation of *m* (A_3O_9) and *n* ($A_3A'O_6$) layers leads to numerous $A_{3m+3n}A'_nB_{3m+n}O_{9m+6n}$ polytypes described by J. M. Perez-Mato *et al.* [22]. A comprehensive list of the $A_{3m+3n}A'_nB_{3m+n}O_{9m+6n}$ compounds is given in [23]. The different stacking sequences of the (A_3O_9) and ($A_3A'O_6$) layers results in different values of c parameter and often leads to an enormous increase, which makes the structure refinement impossible. The composite structure model was first suggested by M. Evain *et al.* [24] and generalized by J. M. Perez-Mato *et al.* [22]. These structures are con-

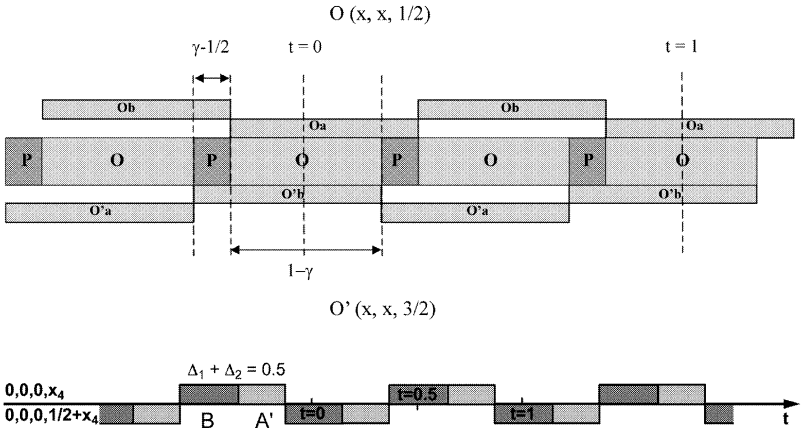

Fig. 10. Top: saw-tooth function domains limiting *t* regions where either octahedral (O) or trigonal prismatic coordination exists; bottom: domains of existence of B and A′ cations.

sidered as consisting of $[(B, A')O_3]_\infty$ and $[A]_\infty$ subsystems with a common *a* parameter, different c_1 and c_2 parameters and a modulation vector defined as $\boldsymbol{q}=\gamma\boldsymbol{c}_1^*$. In general they are commensurate with $\gamma=3(n+m)/2(2n+3m)$, but for members with large denominators it is better to consider the modulation as incommensurate.

Intensities of satellite reflections for modulated structure are rather weak and sometimes could be ignored. Composite structures provide reflections from both sublattices with intensities of the same order of magnitude that should de definitely taken into account. Commensurate structures can be treated as the superstructure, while in the incommensurate case $3+d$ approach is the only way out.

The synthesis and data collection for $Sr_{1.32}Mn_{0.83}Cu_{0.17}O_3$ are described elsewhere [25]. The crystal structure of $Sr_{1.32}Mn_{0.83}Cu_{0.17}O_3$ was refined from X-ray powder diffraction data in $R\bar{3}m(00\gamma)0s$ $(3+1)d$ superspace group with two sets of cell parameters obtained from powder pattern profile analysis and successive least-squares refinement: $a_1=a_2=9.5971(8)$ Å, $c_1=2.60008(17)$ Å, $c_2=3.9312(3)$ Å, thus producing modulation vector $\boldsymbol{q}=0.6616(1)\boldsymbol{c}_1^*$ with interlattice matrices:

$$W^1=\begin{pmatrix}1&0&0&0\\0&1&0&0\\0&0&1&0\\0&0&0&1\end{pmatrix}\qquad W^2=\begin{pmatrix}1&0&0&0\\0&1&0&0\\0&0&0&1\\0&0&1&0\end{pmatrix}$$

The incommensurate composite model for the $A_{3n+3}A'_nB_{n+3}O_{6n+9}$ compounds has been previously discussed, and will be briefly summarized here. The average structure is presented as $[Mn_{0.83}Cu_{0.17}O_3]_\infty$ (Mn, Cu site – 0, 0, 0; O site* – 0.16, 0.16, 1/2) in the first subcell and $[Sr]_\infty$ (Sr site – 1/3, 0, 1/4) in the second one. The Sr content is determined by a volume ratio $V_1/V_2=0.662$, where V_1 and V_2 are cell volumes of the first and second subsystems, respectively. The amount of the A cations determines $\gamma=(1+x)/2$, where *x* is taken from the $A_{1+x}(A'_xB_{1-x})O_3$ formula. The occupancy modulations for Sr, (Mn, Cu) and O atoms are modeled with the saw-tooth functions.

The saw-tooth function with $\Delta=1/2$ and $x_4^0=1/4$ for oxygen atoms with the average coordinates (0.16, 0.16, 1/2) separates them into two sets of atoms related by a mirror plane m_s, Oa and Ob, so that each set forms the (001) triangular face of an octahedron or a trigonal prism. Depending upon the *t* coordinate, the trigonal prismatic sites are created by either Oa–Oa or Ob–Ob combinations, whereas the Oa–Ob combination corresponds to an octahedral site (Fig. 10, top). In the idealized structure model of $A_{3m+3n}A'_nB_{3m+n}O_{9m+6n}$ hexagonal perovskites the width of the octahedron D_O measured along the *c* axis is one half the width of the trigonal prism D_P, however in reality the $D_P=2D_O$ condition is not fulfilled. To overcome this difference a displacement of oxygen atoms along the *c* axis is introduced, which is characterized by the $u_{0,3}(O)=(D_O-D_P)/2$ component ($u_{0,1}(O)$ and $u_{0,2}(O)$ were assumed to be small and fixed to zero). The (Mn, Cu) cations at (0, 0, 0) are separated into two sites, one situated at the B octahedral sites and the other situated at the A′

* The site is half occupied; see the further explanation.

trigonal prismatic sites. Windows of the saw-tooth functions for B and A′ positions should coincide with the t regions where either octahedral or prismatic oxygen environment occurs, that requires $\Delta_B=(1-x)/2$ and $\Delta_{A'}=x/2$ and $x^0_{4,B}=0$, $x^0_{4,A'}=1/4$ (Fig. 10, bottom). By symmetry $u_{0,1}(B, A')=u_{0,2}(B, A')=0$, whereas $u_{0,3}(B)$ and $u_{0,3}(A')$ should result in the same slope of the saw-tooth functions as for oxygen atoms. Hence, $u_{0,3}(B)=(1-x)u_{0,3}(O)$ and $u_{0,3}(A')=xu_{0,3}(O)$. Thus, the distribution of the cations between octahedral and prismatic sites is determined by a single refineable parameter $u_{0,3}(O)$. In the second subsystem, the Sr atoms at (1/3, 0, 1/4) can be located along the c axis either at the level of the centers of the prisms or at the level of the triangular faces. These two subsets are described by saw-tooth functions with $\Delta_{Sr1}=x/(1+x)$, $x^0_{4,Sr1}=0$ and $\Delta_{Sr2}=(1/3)-[x/(1+x)]$, $x^0_{4,Sr2}=1/2$, $u_{0,3}(Sr1)=[3x/(1-2x)]u_{0,3}(Sr2)$.

This model was introduced to the structure refinement taking into account satellite reflections up to second order. The preferred orientation was refined with the March-Dollase function. The initial starting model gave reasonable values of reliability factors ($R_{all}=0.057$, $R_P=0.017$). Due to the small difference in scattering power of Mn and Cu we did not refine the occupancy factors for the B and A′ sites to determine the distribution of these cations. The B site was assumed to be fully occupied by Mn, whereas 53.9% Cu and 46.1% Mn were placed at the A′ site to achieve the nominal phase composition. After the initial refinement step large value of atomic displacement parameter for the A′ cation ($U_{iso}=0.024$ Å^2) was observed. The A′ cations were displaced from their ideal position (0, 0, 0) to a (x, x, 0) position, that means a shift of these cations towards one of the rectangular faces of the trigonal prism. This shift results in a two times decrease of the atomic displacement parameter for these atoms, followed by a decrease of the reliability factor to $R_{all}=0.049$. Further improvement of the fit was achieved by adding one harmonic component of the positional modulation function to the saw-tooth displacement of the B cations. Prior to that, the orthogonalization procedure was performed for the modulation functions of the B cations [26]. The final values of the reliability factors $R_{all}=0.044$, $R_P=0.016$ reflect the good agreement between calculated and experimental profiles (Fig. 11).

Let us consider the chemical formula $A_{1+x}A'_xB_{1-x}O_3$, where $x=p/q$, where p and q are coprime numbers. If N_{prism} and N_{oct} are respectively the numbers of trigonal prismatic and octahedral cavities in $[(B, A')O_3]_\infty$ chains, then the ratio $N_{prism}/N_{oct}=x/(1-x)=p/(q-p)$. $BaNiO_3$ [27] ($N_{prism}=0$, $N_{oct}=1$, consequently $p_1=0$, $q_1=1$) (Fig. 9a) and Sr_4PtO_6 [28] ($N_{prism}=1$, $N_{oct}=1$, consequently $p_2=1$, $q_2=2$) (Fig. 9b) can be taken as parent structures. The combination of these structures will produce a new structure with

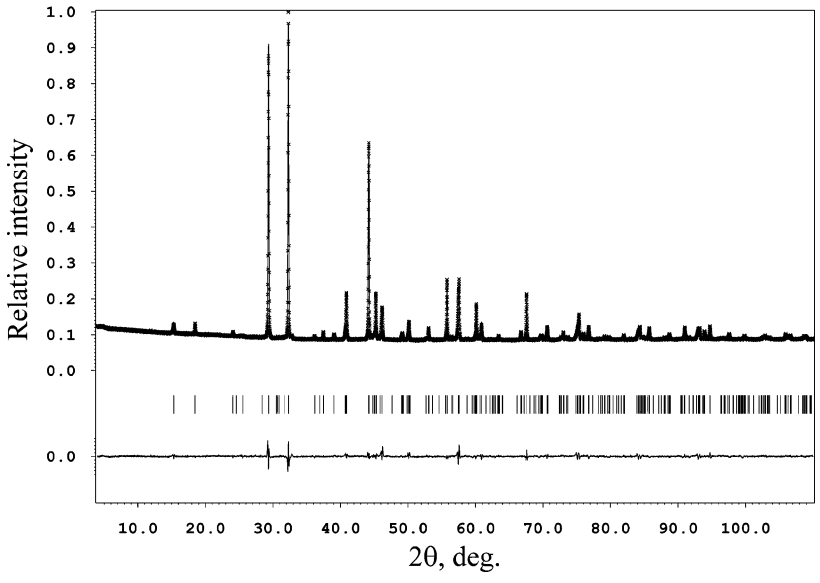

Fig. 11. Experimental, calculated and difference X-ray diffraction profiles for $Sr_{1.32}Mn_{0.83}Cu_{0.17}O_3$.

$p/q=(p_1+p_2)/(q_1+q_2)=1/3$. This is the structure of the commensurate $Sr_{4/3}Mn_{2/3}Cu_{1/3}O_3$ phase ($N_{prism}=1$, $N_{oct}=2$, consequently $p_3=1$, $q_3=3$). The process is continued to infinity, giving rise to enormous number of phases as described by Farey tree [22]. For $Sr_{1.32}Mn_{0.83}Cu_{0.17}O_3$ the refined value of $\gamma=0.6616(1)$ corresponds to $x=0.3232$. It is close to $p/q=1/3$, where p is the number of prisms in the chains and $(q-p)$ is the number of octahedra. Using Farey tree [22], the fractional value $p/q=32/99=0.3232$ for x can be found. Expressing p/q through the preceding "generators" p_1/q_1 and p_2/q_2, so that $p/q=(p_1+p_2)/(q_1+q_2)$ the sequence of octahedra and prisms can be found. Thus, the repeat period along the chains comprises 99 polyhedra according to the sequence $1\times(3\,oct+1\,prism)+9\times(2\,oct+1\,prism)+1\times(3\,oct+1\,prism)+10\times(2\,oct+1\,prism)+1\times(3\,oct+1\,prism)+10\times(2\,oct+1\,prism)$. Such polyhedral arrangement was confirmed by high resolution electron microscopy [25].

6. Concluding Remarks

The intrinsic one-dimensional character of powder XRD pattern results in a significant loss of structural information if compared with the single crystal X-ray diffraction technique. A lack of data seems to be crucial for possibility to determine *ab initio* the structure model for an incommensurate modulated compound using powder XRD data as a unique source of information. However, compared with other techniques such as electron diffraction and high-resolution electron microscopy, powder XRD patterns of incommensurate phases become applicable not only for phase analysis, but also for determination and precise refinement of the unit cell metrics, modulation vector and possible superspace group. If an appropriate model is available from a similar known structure or from chemical considerations, Rietveld refinement appears to be able to provide sensible information on modulation parameters and shed light on peculiarities of the structural organization of composite structures.

Acknowledgement

This work was partially supported by Russian Foundation of Basic Researches (grant No.03-03-32610) and International Centre of Diffraction Data (grant APS 91-05). The authors thanks Dr. V. Petriček for very fruitful discussion and P. Chizhov for help in the paper preparation. Acknowledgement is made to the donors of the American Chemical Society Petroleum Research Fund for the partial support of the research.

References

[1] De Wolff P. M., *Acta Cryst.* **A30** (1974), 777.
[2] *International Tables for Crystallography*, Kluwer Academic Publishers, London, 1999, vol. C. 899.
[3] Petricek V., Gao Y., Lee P., Coppens P., *Phys.Rev. B* **42** (1990), 387.
[4] Van der Lee A., Evain M., Monconduit L., Brec R., Rouxel J., Petricek V. *Acta Cryst.*, **B50** (1994), 119.
[5] De Wolff P. M., Janssen T., Janner A., *Acta Cryst.* **A37** (1981), 625.
[6] Van Smaalen S., *Physical Review B*, **43** (1991), 11331.
[7] Akselrud L. G., Grin Yu. N., Zavalij P. Yu., Pecharsky V. K., Fundamentsky V. S., Thes. report on 12-th ECM, Moscow, 1989, p. 155.
[8] Michel C., Hervieu M., Borel M. M., Grandin A., Deslandes F., Provost J., Raveau B., *Z. Phys.*, **B68** (1987), 421.
[9] Zandbergen H. W., Groen W., Mijoff F. C., Van Tendeloo G., Amelinckx S., *Physica C*, **153** (1988), 602.
[10] Hadermann J., Khasanova N. R., Van Tendeloo G., Abakumov A. M., Rozova M. G., Alekseeva A. M., Antipov E. V., *J. Solid State Chem.*, **156** (2001), 445.
[11] Gao Y., Lee P., Coppens P., Subramanian A., Sleight A. W., *Science*, **241** (1988), 954.
[12] Petricek V., Gao Y., Lee P., Coppens P., *Phys. Rev. B*, **42** (1990), 387.
[13] Mironov A. V., Coppens P., Khasanova N. R., Antipov E. V. Petricek V., *J. Solid State Chem.*, **109** (1994), 74.
[14] Yamamoto, A., Takayama-Muromashi, E., Izumi, F., Ishigaki, T. Asano, H., *Physica C*, **201** (1992), 137.
[15] Gao Y., Coppens P., Cox D. E., Moodenbaugh A. R., *Acta Cryst. A*, **49** (1993), 141.
[16] Khasanova N. R., Mironov A. V., Antipov E. V., *Powder Diffraction*, **10** (1995), 1.
[17] Khasanova N. R., Antipov E. V., *Physica C*, **246** (1995), 241
[18] Petricek, V., Dusek, M. *The crystallographic computing system JANA2000*. Institute of Physics, Praha, Czech Republic, 2000.
[19] Dusek M., Petricek V., Wunschel M., Dinnebier R. E., van Smaalen S., *J. Applied Cryst.*, **34** (2001) 398.
[20] Leligny, H., Durcok, S., Labbe, P., Ledesert, M.. Raveau, B., *Acta Cryst.*, **B48** (1992), 407.
[21] Mironov A. V., Antipov E. V., *High-temperature Superconductors and Novel Inorganic Materials engineering*, Book of Abstracts, MSU-HTSC V conference, March 24–29, 1998, Moscow, Russia, W-21.
[22] Perez-Mato J. M., Zakhour-Nakhl M., Weill F., Darriet J., *J. Mater. Chem.*, **9** (1999) 2795.
[23] Stitzer K. E., Darriet J., zur Loye H.-C., *Current Opinion in Solid State and Materials Science*, **5** (2001) 535.
[24] Evain M., Boucher F., Gourdon O., Petricek V., Dusek M., Bezdicka P., *Chem. Mater.*, **10** (1998) 3068.
[25] Abakumov A. M., Mironov A. V., Govorov V. A., Lobanov M. V., Rozova M. G., Antipov E. V., Lebedev O. I., Van Tendeloo G., S*olid State Science*, **5** (2003) 1117.
[26] Petricek V., van der Lee A., Evain M., *Acta Cryst.*, **A51** (1995) 529.
[27] Takeda Y., Kanamuru F., Shimada M., Koizumi M., *Acta Cryst.*, **B32** (1976), 2464.
[28] Randall J. J., Katz L., *Acta Cryst.*, **12** (1959), 519.